World Journal of Pharmaceutical Sciences
ISSN (Print): 2321-3310; ISSN (Online): 2321-3086
Published by Atom and Cell Publishers
Available online at: http://www.wjpsonline.org/
Original Article

Effect of purified α-mangostin from mangosteen pericarp on cytotoxicity, cell cycle arrest and apoptotic gene expression in human cancer cells

Primchanien Moongkarndi[1,*], Nattapon Jaisupa[2], Nuttavut Kosem[3], Julaporn Konlata[1], Jutima Samer[1], Kovit Pattanapanyasat[4] and Ekkarat Rodpai[5]

[1]Department of Microbiology, Faculty of Pharmacy, Mahidol University, Bangkok, Thailand.
[2]Department of Pharmacology, Phramongkutklao College of Medicine, Bangkok, Thailand.
[3]Innovation Center for Medical Redox Navigation, Kyushu University, Fukuoka, Japan
[4]Center of Excellence for Flow Cytometry, Office for Research and Development, Faculty of Medicine, Siriraj Hospital, Mahidol University, Bangkok, Thailand
[5]Institute of Molecular Biosciences, Mahidol University, Bangkok, Thailand

Received: 17-05-2015 / Revised: 23-06-2015 / Accepted: 06-07-2015

ABSTRACT

α-Mangostin from pericarp of *Garcinia mangostana* L. was purified and investigated on the anti-perliferation, anti-cancer activity on apoptotic-related gene expression and cell cycle arrest against human cancer cells. α-Mangostin was identified by ^{13}C-NMR, DEPT 135-NMR, IR and MS. The peak of α-mangostin from HPLC chromatogram was monitored at 316 nm and displayed at retention time 20.9 minute. Ten human cancer cells showed the cytotoxicity by MTT assay after exposure to α-mangostin. Real-time RT-PCR was used to measure the apoptotic-related genes expression and flow cytometer was performed to analyze the cell cycle arrest. The ED_{50} on cytotoxicity of α-mangostin obtained from 5 breast cancer cells were between 8.21-15.41 µg/ml; from 2 ovarian cancer cells were 8.15-33.4 µg/ml; from 1 liver hepatocellular carcinoma cell was 6.12±0.32 µg/ml and from 2 colon cancer cells were 8.63-18.98 µg/ml. The Bax/Bcl-2 ratios were increased in all cancer cells suggested that it might induce cell death by apoptotic pathway. α-Mangostin demonstrated at G0/G1 phase cell cycle arrest by flow cytrometric analysis. α-Mangostin showed anti-proliferation activities to all 10 cancer cells. This compound should be further investigated for understanding the mechanisms of action and *in vivo* model study to justify that α-mangostin is effective for prevention and treatment of cancers.

Key Words: α-mangostin, mangosteen, validation method, cytotoxicity, cancer, cell cycle, Bax/Bcl-2 ratio

INTRODUCTION

Garcinia mangostana L. (mangosteen), belonging to family Guttiferae, is an evergreen plant widely found in the tropical countries including Thailand. The pericarp of the fruit has been used as a folk medicine for many years to treatment of skin infection, wound and dysentery diarrhea [1]. It has been revealed to have major biological active compounds, α- and γ-mangostin, and other minor xanthones [2]. Among these compounds, α-mangostin is one of the interesting constituent, which generally found in various parts of this plant especially in the pericarp which was thrown away after taken the meat of the fruits. α-Mangostin has been reported to possess interesting pharmacological activities, such as anti-vancomycin resistant *Enterococci* [3], induction apoptosis of human leukemia [4], inhibition the oxidation modification of human LDL [5], histamine H1 receptor antagonist [6], anti-MRSA[7] and effect on Ca^{2+}-ATPase [8] [9]. In addition, anticancer of this compound is increasingly interesting. A number of studies reported anticancer both *in vitro* and *in vivo* studies. For example, α-mangostin showed the inhibition of human malignant glioblastoma growth by 50%, decrease human prostate carcinoma and human colon adenocarcinoma growth, as well as induced apoptotis of several cancer cells lines. Moreover, it can inhibit chemically-induced cancer from 1,2 dimethylhydrazine in colon cancer model [10]. Physically, α-mangostin is a yellow solid with the melting point 181.6-182.6 °C[11]. Its IUPAC name is 1,3,6-trihydroxy-7-methoxy-2,8-bis-(3-methyl-2-butenyl)-9-xanthenenone [12] or 1,3,6-

***Corresponding Author Address:** Primchanien Moongkarndi, Department of Microbiology, Faculty of Pharmacy, Mahidol University, Bangkok, Thailand.* **primchanien.moo@mahidol.ac.th**

trihydroxy-7-methoxy-2,8-bis-(3-methyl-2-butenyl)-9*H*-xanthen-9-one or 1,3,6-trihydroxy-7-methoxy-2,8-di(3-methyl-2-butenyl) xanthone. The empirical formula of this compound is $C_{24}H_{26}O_6$ with molecular weight at 410.46 (Figure 1). It is the hydrophobic compound which is practically insoluble in water but soluble in alcohol, ether, acetone, chroloform and ethyl acetate. The UV absorption maxima (λ_{max}, in ethanol) were recorded at 243, 259, 318 and 351 nm (log ε 4.54, 4.44, 4.38 and 3.86) [11].

α-Mangostin is an enriched xanthone in mangosteen pericarp and could be isolated by various phytochemical procedures [13-15]. In principle, the evaluation of anticancer drugs has a vast varieties of assays to performed and summarized the overall activities.

To determine the effect on changes in certain gene related to apoptotic pathway was performed to ensure the role of α-mangostin on anticancer. The B-cell lymphoma 2 (Bcl-2) is recognized as a type of multidrug-resistant protein that protects tumor cells from the cytotoxic effects of virtually every anticancer drug. The other regulator of cellular responsiveness is the pro-apoptotic molecule Bcl-2-associated X protein (Bax). Whereas Bcl-2 over-expression has been shown to inhibit apoptosis, a predominance of Bax to Bcl-2 accelerates apoptosis upon apoptotic stimuli [16, 17]. Bcl-2 and Bax interactions have often been presented as a model where the cell's fate can be changed by changing the balance or ratio of Bax and Bcl-2 protein expression. It has been suggested that the Bax/Bcl-2 ratio may be observed to determining apoptosis in cancer cells [18].

This study aimed to isolate, purify, elucidate the structure of α-mangostin and validate the assay method by HPLC analysis. Additionally, studies on the cytotoxic effect against 10 cancer cell lines, cell cycle arrest analysis and changes in apoptotic gene expression of Bax/Bcl-2 ratio by this compound were determined.

MATERIALS AND METHODS

Plants: Mangosteen was collected from Chantraburi, the eastern province in Thailand. Fruits were cleaned with running tap water and fresh pericarp were separated and chopped into pieces, dried and milled into powder.

Extraction, isolation and structure elucidation of α-mangostin: The process on α-mangostin isolation was previously described [19]. Briefly, mangosteen powder (1 kg) was macerated with ethanol (EtOH) at 60°C for a week. The crude extract was then filtered through Whatman No.1 filter paper under vacuum. The filtrate was concentrated by evaporation with a vacuum rotary evaporator at 45°C to yield crude EtOH. EtOH extract was partitioned with ethyl acetate (EtOAc) to yield low polar constituents. Supernatants were collected and evaporated at 45–60°C to obtain EtOAc extract. This EtOAc-soluble part was chromatographed on a silica gel column chromatography and eluted with gradient solvent system by gradually increase the polarity (hexane, hexane-EtOAc, EtOAc, EtOAc-MeOH, MeOH). The fractions composed of α-mangostin, visuallized by thin layer chromatograpy (TLC), were pooled and rechromatographed with the same solvent system. The obtained yellow powder of the isolate was crystallized. The physicochemical properties of the purified α-mangostin obtained were identified and confirmed by the melting point, UV spectroscopy, and ^{1}H-NMR ^{13}C-NMR, DEPT 135-NMR, IR and MS spectra.

Cell lines: Five human breast cancer cell lines (SKBR3, BT549, BT474, MCF7, MDA-MB-231), two human ovarian cell lines (OVCAR3, SKOV3), two human colon cell lines (CACO-II, SW620), and one human hepatocellular carcinoma cell line, HepG2, were obtained from ATCC. The cells were cultured in RPMI-1640 medium (Gibco, Grand Island, NY, USA) supplemented with 10% heat-inactivated fetal calf serum (FBS; Gibco).

The status of HPLC instrument: HPLC instrument (Shimadzu, Japan) with: pump (LC-10 ADVP), degasser (DGU-12A), detector (SPD-M10Avp UV-Vis photodiode array), system controller (SCL-10AVP), injector (Rheodyne 7725) and column (BDS HYPERSIL C 18 size 250 mm L x 4.6 mm i.d., 5 μm particle size Guard column: Bondapack C 18). The mobile phase consisted of 0.1 % *o*-phosphoric acid in de-ionized water and acetonitrile which applied in the gradient elution. The flow rate was adjusted to 1 ml/min. The temperature was held constant at 25°C. Ultraviolet spectra were recorded. The data was analyzed by LC-MS solution software.

Preparation of standard solution and calibration curve: The stock of standard α-mangostin solution was prepared at the concentration of 1,000 μg/ml by dissolving in methanol (MeOH), then diluted into 500, 250, 100, 25, 10 and 5 μg/ml respectively. To construct the calibration curve, 5 μl of each concentration were injected in triplicate to HPLC instrument. The average peak areas of each concentration were plotted against the correct concentration. The square of correlation coefficient and equation of linear regression were calculated.

Accuracy test: The standard α-mangostin at 50, 100 and 200 µg respectively were added into the purified samples and triplicate analyzed the quantities as the % recovery. The acceptable value is ranged between 80 to 120 %.

Precision test: Precision experiments are classified into intra-day and inter-day and calculated as the relation standard deviation (RSD). The data used to perform RSD of intra-day precision is the areas of six injections separately in the same day and the data for inter-day is the areas of six injections in three days. The acceptable value is less than 15 %

Limit of detection: Limit of detection is the lowest concentration of an analyze that can be detected, not quantitated, based on three times of signal-to-noise ratio (S/N = 3).

Limit of quantitation (LOQ): Limit of quantitation is the lowest concentration of an analyze that can be determined with acceptable precision and accuracy under the stated operational conditions of the method based on ten times of signal-to-noise ratio (S/N = 10).

Cytotoxicity assay (MTT assay): Cytotoxicity was determined based on MTT assay. To obtain anti-proliferative results, ten cancer cell lines were incubated with α-mangostin and standard drugs; Doxorubicin, Paciltaxel, Cisplatin, Methotrexate and Mitomycin C used for each cancer type therapy were simultaneously performed as positive controls. The experiment was performed by modified from the method described previously [20]. Briefly, 100 µl at 1 X 10^4 cells of each cell line were plated into 96-well plate. The cells were then incubated with each compound at various concentrations by two-folded dilution starting from 50 to 2.5 µg/ml. The plates were further incubated at 37 °C with 5% CO_2 for 24 h. After removal of incubated supernatant, 50 µl of 1 mg/ml MTT solution was added and further incubated for 2 h. The formazan, product from the assay, was further dissolved by adding isopropanol and measured by microplate reader at 570 nm. The experiment was operated in triplicate. The cell viability was calculated by the following equation.

Cell viability (%) = $((A_{sample} - A_{blank}) / (A_{negative\ control} - A_{blank})) \times 100$

Cell cycle analysis: KOV3 cells (1.5 x 10^6 cells/10 ml) were plated into each well of 24-well plate and incubated for 24 h before exposure with samples for appropriated incubating time [21]. Cells were harvested and washed with PBS. The cell pellets were collected after centrifugation at 2,500 g. for 5 min and then fixed in 1 ml of 70% ice-cool ethanol. Then, ethanol was descanted. DNA extraction buffer was added into tubes and incubated at 37 °C for 30 h before resuspending in dye solution to stain DNA at 25 °C for 15 min in the dark. DNA contents were measured with flow cytometer.

RNA extraction from cell line: The total cellular RNA from ten cancer cell lines were treated with α-mangostin at the concentration of ED_{25}, ED_{50} and ED_{75} calculated from the MTT assay from each cell line, standard anticancer drugs; Taxol as positive control and un-treated cell lines as negative control were extracted with Guanidinium Phenol-Chloroform method. Briefly, treated cells grown in monolayer cultures were collected and suspended with 1 ml of denaturing solution and homogenized by vortex mixing. After homogenization, 0.1 ml of 2 M sodium acetate (pH 4.0), 1 ml of saturated phenol (pH 5.2) and 0.2 ml of CIA mixture (49:1 v/v) were added subsequently. The mixture was incubated on ice for 15 min and centrifuged at 10,000 rpm (Mikro 22R / Hettich) for 20 min at 4°C. The aqueous phase was collected into a fresh tube and then precipitated with isopropanol to obtain RNA. The RNA pellet was dissolved in DEPC-treated water and kept at -80°C until needed.

Real-time RT-PCR: The quantification of the selected genes by real-time RT-PCR was performed using Mx3000P qPCR System (Agilent Technologies, USA) with the primers shown in Table 1. Every reaction consisted of 2 µl cDNA, 1 µl of each primer (400 nM) and 21 µl reaction buffers (GoTaq 1-Step qRT-PCR, Promega, US) (total reaction volume 25 µl) (Invitrogen). Real-time PCR cycles consisted of: 30 minutes at 50°C, 5 minutes at 95°C for polymerase activation, 35 cycles of 30 seconds at 95°C (denaturation) 30 seconds at 55°C, 30 seconds at 72°C (annealing and extension). β_2 microglobulin (β_2m) of each sample served as intrinsic control. The threshold cycle (CT) of each sample was normalized to human β_2m. The analysis uses the sample's crossing point, the efficiency of the reaction, the number of cycles completed and other values to compare the samples and generate the ratios. The results are expressed as a normalized ratio.

RESULTS

Extraction, isolation and structure elucidation of α-mangostin: The product was obtained as a yellow solid at the yield of approximately 2 % of dry powder from pericarp. The purity was more than 95 % by HPLC analysis. The melting point was recorded at 179-180 °C. The UV spectrum scanning from 210–370 nm presented the λ_{max} at 242 and 316 nm and the shape of this UV chromatogram was similar to that of α-mangostin

in the report of Ji, *et al* [1] (Figure 2). The molecular formula of $C_{24}H_{26}O_6$ was established on the basis of its mass spectrum ($[M]^+$ at *m/z* 339.2). The IR absorption bands exhibited the presence of O-H, C=O, C=C aromatic, C-O, CH_2 and CH_3 groups (Table 2).

From NMR spectra, ^{1}H-NMR data were compared to those of α-mangostin [12], singlet peak at δ_H = 6.183 and 6.339 ppm were assigned to OH group (H-3 and H-6). The δ_H = 3.816 ppm belongs to H in 7-OCH_3 group. Two aromatic protons (H-4 and H-5) were detected at δ_H = 6.28 and 6.82. The doublet peak at δ_H = 4.097 ppm (*J* = 6.4 Hz) and 3.462 ppm (*J* = 7.2 Hz) were presented for H-11 and H-16 respectively. H on four methyl groups of position 14, 15, 19 and 20 exhibited the multiplet peaks between 1.701 to 1.854 ppm. H-12 and H-17 showed the peaks in the range of 5.256 to 5.318 ppm. These data were summarized in Table 3. ^{13}C-NMR spectrum showed 24 signals due to two prenyl side chain (10 carbons), xanthone skeleton (13 carbons) and 7-OCH_3 (1 carbon). Each chemical shift value was assigned to each carbon by comparing to those of mangostenone C, D, E and dimethylmangostin[14] (C-2 prenyl substituent, C-8 prenyl substituent and xanthone skeleton) [22] [23]. The chemical shift values of ^{13}C-NMR spectrum were summarized in Table 4. From DEPT 135-NMR, two inverted peaks (δ = 27.206 and 22.082 ppm) were assigned for two methylene (CH_2) groups in the molecule (data not shown).

Validation method: The pure peak of α-mangostin from HPLC analysis which was monitored with a UV detection at 316 nm performed at the retention time 20.9 minute (Figure 3). The calibration curve was constructed to investigate the linearity resulting the correlation coefficient (r^2) at 0.9998. The % recovery was obtained in the range between 99.5-102.0 %. The RSD of intra-day and inter-day were obtained at 1.5-2.8 % and 2.0-5.4 % respectively. These data indicate that the linearity, accuracy and precision were acceptable. The LOD and LOQ were recorded at 0.3 μg/L (S/N = 3) and 1.0 μg/L (S/N = 10) respectively. The data were summarized in Table 5.

Cytotoxicity assay: A viability of all cell lines after exposure to α-mangostin was demonstrated as line graph (Figure 4). The summary of ED_{50} of five cytotoxic agents and α-mangostin was shown in Table 6 as mean±SD. α-Mangostin showed both superior and inferior results when compared with standard compounds. Almost of cancer cell lines were susceptible to doxorubicin and paclitaxel, except methotrexate. Only CACO-II, human epithelial colorectal adenocarcinoma cells, was resistant to all cytotoxic agents, but it was susceptible to α-mangostin (Table 6).

Cell cycle analysis: DNA content and distribution in normal cells, different stages of cells and cell death can measure by flow cytometry. The impact of α-mangostin on the cell cycle was examined against SKOV3 cell lines. The DNA content of cells was demonstrated in Table 7. The α-mangostin could arrest cell cycle at G0/G1 phase on SKOV3 of dose 25 μg/ml at various times. SKOV3 cells were exposed with 25 μg/ml of α-mangostin for indicated time and analyzed using flow cytometer. Values were presented as mean±S.D. (*n* = 3).

Bax/Bcl-2 ratio: The presence of both Bax mRNA and Bcl-2 mRNA confirmed that Bax and/or Bcl-2 were actively produced in 10 cancer cell lines. The Bax/Bcl-2 ratios of the mRNA and protein levels were shown in Figure 5. The results were compared the treated cancer cells with cells treated with α-mangostin at various concentrations and with Taxol, an anticancer drug as control. The results showed that the Bax/Bcl-2 ratios were increased in all cancer cell lines. SKBR3, MCF7, OVCAR3, Hep-G2, Caco II and SW620 cells were increased related to the concentrations of α-mangostin but in BT549, BT474, MD-MB-231 and SKOV3 cells were not related. In our study, the cancer cells were also observed the changing in cell morphology under Microscope and found the apoptotic death cells occurring related to the concentrations of treated α-mangostin. The results suggested that α-mangostin might induce cell death in cancer cell by apoptotic pathway.

DISCUSSION

In our present study, we aimed to develop the isolation process of α-mangostin from the pericarp of mangosteen and set up the method validation of HPLC analysis to determine this compound. The extraction and purification were simple by soxhlet apparatus and column chromatography. The characters were confirmed by the tests previously mentioned in extraction, isolation and structure elucidation section. The data from ^{1}H-NMR, UV spectra and the melting point were directly compared to the reports previously published [1] [11] [24]. The chemical shift values from ^{13}C-NMR were assigned to each carbon atom by comparing to those of mangostenone C, D, E and dimethylmangostin which only differed from α-mangostin in the native of the constituents on the xanthone nucleus (C-2, C-6 and C-8 substituents) [22] [23]. According to the melting point, UV and ^{1}H-NMR spectral data, these evidences agreed with the references. DEPT 135-NMR showed two

inverted peaks signaling to two methylene groups which supported the chemical structure of this compound. MS and IR spectral data also supported the characters of this isolated compound to be α-mangostin. The purity over than 95% was calculated from the peak area ratio of HPLC chromatogram of three injections (data not shown). Validation study of the analytical method is a necessary step to assay novel compounds and must ensure that the obtain detection provide the repetitive and accurate results. It is generally accepted that the accuracy which result in term of % recovery must be in the range of 80 to 120% and the RSD which represents the precision must not be over than 15%. The HPLC chromatogram exhibited a pure narrow and sharp peak of α-mangostin that completely separated from the others. This indicated that the mobile phase system was suitable. The data from method validation showed good and acceptable linearity, precision and accuracy, therefore, this developed method was ensured to assay this compound. From the outcomes of LOD and LOQ, we have proven that α-mangostin can be detected and quantitated by HPLC assay under these conditions at the concentration of 0.3 and 1.0 µg/L respectively.

Although the commercial α-mangostin is available, but to obtain high quality and high amount within time frame and with simple equipment is of importance, especially for *in vivo* study and future clinical application. α-Mangostin isolated from the pericarp will elevate the value of the waste product of mangosteen. We are now on *in vivo* studying the application of α-mangostin for toxicity and antitumor activity. The developed method is very helpful to obtain high yield and high purity of α-mangostin from pericarp and any part of mangosteen tree.

In addition, we also performed the cytotoxic effect of this compound against ten cancer cell lines and compared to standard cytotoxic agents as shown in Table 6. Several studies reported the anti-proliferative and cytotoxic effects of α-mangostin against several cancers both *in vivo* and *in vitro* studies [10]. From our result, the susceptibility to α-mangostin was different among these cell lines when compared to anti-cancer agents. Akao, *et al* showed the inferior anticancer effect of α-mangostin comparing to standard drug on human colon cancer DLD-1 cells [25], however, α-mangostin showed the better cytotoxic effect than standard agents in some cell lines in our study (Table 6). Therefore, α-mangostin still possesses effective anti-proliferation and cytotoxic properties and needs more details of study for a suitable future application. The development and application of this compound to synergistically treated cancer was shown to give a clinical benefit. For example, the combination of α-mangostin and 5-FU for cancer therapy showed the synergistic effect [25], and α-mangostin showed the enhancement the cytotoxic effect of betulinic acid, whereas the preventive property was observed in cisplatin treatment in HCT 116 colorectal carcinoma cells [26]. α-Mangostin inhibited cellular growth and proliferation via numerous molecular mechanisms. For example, it induces cell death by apoptotic process, inhibits the cellular proliferation by interfere with Akt and MAPK pathway and trigger cell cycle arrest at G1 phase [27] [25]. It can induce apoptosis through both extrinsic and intrinsic pathway [25] [28] [29].

The cell cycle machinery and components of check-point pathways have already provided a wealth of targets for novel anticancer drugs. Many of compounds under study as anti-tumor agents act at multiple steps in the cell cycle, and their effects may be cytostatic or cytotoxic, depending on the cell cycle status of the target cells. Hence, an understanding of the molecular interactions involved may suggest ways to sensitize cells to the effects of these compounds. In particular, combinations of drugs, applied in a specific sequence, may be used to fight a tumor cell population into a state where it is most susceptible to cytotoxic effects of novel, or indeed traditional, chemotherapeutic agents [30]. In this study, we analyzed the effect of α-mangostin on cell cycle of SKOV3 cells. As compared to control, cell cycle analysis revealed the accumulation of cells in G0/G1 phase upon treatment with 25 µg/ml of α-mangostin in the time course from 57.11% of untreated control cells at 0 h to 75.0% of 3-h treated cells. While cell population was declined in S and G2/M phases (Table 7). The important mechanism may be related to the inhibitory activity on cyclin dependent kinases (CDKs) control most of the major cell-cycle transitions of eukaryotes. The CDKs associated with the G1/S phase transition in mammalian cells are CDK2, CDK4 and CDK6. Activities of these CDKs are influenced by multiple layers of regulation, including the availability of cyclins, phosphorylation and dephosphorylation of CDKs, and CDK inhibitors [31]. The treatment of α-mangostin may inhibit CDK activities and result in cell-cycle arrest at the G0/G1 phase of SKOV3 cells.

One study used MDA-MB-231 cell line treating with α-mangostin and found out any mechanisms by which the cell was killed[28]. This study may indicate that this cell line seemed susceptible to α-mangostin, and it was consistent to our study that MDA-MB-231 cell line was susceptible to this

compound. Methanolic extract of mangosteen peel showed the anti-proliferative effect against SKBR3 cell line [32] and obtained antitumor effect in BALB/c mice transfected with NL-17 cells [33]. Our recently study may suggest that α-mangostin existing in crude methanolic extract played that remarked role.

To study on changes of apoptotic gene expression, the Bcl-2 family comprises of both pro-apoptotic and anti-apoptotic proteins with opposite effects on mitochondria. Anti-apoptotic members include Bcl-2, Bcl-xL, Bcl-W, Mcl-1, whereas pro-apoptotic members are Bid, Bax, Bakm, Bmf and others [34, 35]. Several pathways involve p53-mediated apoptosis, and one of these is the Bcl-2 and Bax proteins. The Bax protein is a p53 target and known to promote cytochrome c release from mitochondria which in turn activates caspase-3 [36, 37]. The results showed that the Bax/Bcl-2 ratios were increased in all cancer cell lines, suggested that α-mangostin might induce cell death in cancer cell by apoptotic pathway.

According to our obtained result, α-mangostin looks interesting and has a good trend to develop as an anti-cancer agent due to its cytotoxic property. Additionally, many types of cancer become resistant to their standard therapies but not α-mangostin, for example, all of cancer types resisted to methotrexate. Doxorubicin is commonly administered in all cancer types mentioned in this study and CACO-II seems to resist to it. In case of MDA-MB-231, α-mangostin showed the higher potency than every cytotoxic agent, except paciltaxel. α-Mangostin showed greater potency than mitomycin C in almost cancer types. In overall, α-mangostin performed higher, lower, and equal potency comparing to modern agent depending on cell types. Studies of pharmacokinetics and pharmacodynamics have been reported increasingly [10] [38] [39]. Therefore, α-mangostin can be a natural candidate and further developed to be a novel pharmaceutical product for treatment cancer. We are certain that the intensive study of modifying the molecular substituents, clinical trial and pharmaceutical formulation will lead the way of useful novel medicine development.

CONCLUSION

The α-mangostin is derived from the plant as well as possesses a pharmacologically valuable benefit. Therefore, it has a good trend to be developed to a suitable form and can be a candidate in cancer therapy. It may be used instead of modern drugs or in combination with modern drugs. This may be helpful to enhance the efficacy as well as reduce in some unwanted side effect of standard therapies due to its origin from natural product. We hope that α-mangostin can be further developed to be a novel product and truly used in cancer therapy.

ACKNOWLEDGEMENT

This study was financially supported by NRCT of the year 2013 and 2014. We also gave a special thanks to Mr. Narongchai Pongpan for his kind assistance for the purification and identification of the isolates.

Table 1 List of primers used in this study for RT-PCR

Gene	Primers
Bcl-2 [40]	5'-CTACGAGTGGGATGCGGGAGATG-3'
	5'-GGTTCAGGTACTCAGTCATCCACAG-3'
Bax [40]	5'-ACCAAGAAGCTGAGCGAGTGTC-3'
	5'-TGTCCAGCCCATGATGGTTC-3'
$h\beta_2m$	5'-CTT GTC TTT CAG CAA GGA CTG G-3'
	5'-CCT CCA TGA TGC TGC TTA CAT GTC-3'

Table 2 IR spectral data of α-mangostin

Functional groups	Wave number (cm^{-1})	
OH	3260	stretching
C=O	1643	stretching
C=C aromatic	1609, 1583	stretching
C-O	1223	stretching
CH_2	2965	stretching
CH_3	2962	stretching
CH_3	1454	bending

Table 3 ^{1}H-NMR spectral data*

H Position	Chemical shift value in ppm
H-3	6.183 (*s*)
H-4	6.295 (*s*)
H-5	6.827 (*s*)
H-6	6.339 (*s*)
H-11	4.097 (*d*, *J* = 6.4 Hz)
H-16	3.462 (*d*, *J* = 7.2 Hz)
H-12, H-17	5.285 (*m*)
H-14, H-15, H-19, H-20	1.847 (*dd*, *J* = 0.8 Hz, 0.8 Hz), 1.7815 (*d*, *J* = 1.2 Hz), 1.7025 (*d*, *J* = 1.2 Hz)
7-OCH_3	3.816 (*s*)

*Measured at 400 MHz in $CDCl_3$ and TMS was used as an internal standard

Table 4 ^{13}C-NMR spectral data*

C Position	Chemical shift value in ppm
C-1	161.234
C-2	109.086
C-3	162.241
C-4	93.944
C-4a	156.418
C-5	102.193
C-6	155.702
C-7	143.196
C-8	137.680
C-8a	112.847
C-9	182.666
C-9a	104.270
C-10a	155.159
C-11	27.205
C-12	122.075
C-13	136.418
C-14	26.440
C-15	18.849
C-16	22.084
C-17	123.787
C-18	132.777
C-19	18.542
C-20	26.468
7-OCH_3	62.694

*Measured at 100.6 MHz in $CDCl_3$ and TMS was used as an internal standard

Table 5 Data of the validation method

Experiments	**Results**
1. Linearity [Correlation coefficient (r^2)]	0.9998
2. Accuracy (% Recovery)	99.5-102.0
3. Precision (RSD)	
Intra-day	1.5-2.8
Inter-day	2.0-5.4
4. Limit of detection (LOD, S/N = 3)	0.3 µg/L
5. Limit of quantitation (LOQ, S/N = 10)	1.0 µg/L

Table 6 The summary of ED_{50}±SD of cytotoxic drugs and α-mangostin against viability of all tested cancer cell lines

Cell lines	Doxorubicin	Paciltaxel	Cisplatin	Methotrexate	Mitomycin C	α-mangostin
SKBR3	2.43±0.03	1.20±0.00	9.83±0.20	>400	19.46±1.29	8.21±0.37
BT549	1.50±0.05	1.20±0.03	7.01±0.25	>400	26.97±1.63	6.09±0.39
BT474	2.27±0.22	13.39±0.22	27.18±0.55	>400	18.41±1.39	15.41±0.67
MCF-7	1.82±0.90	25.34±1.48	36.46±1.31	>400	14.32±1.25	10.19±0.43
MDA-MB-231	30.50±5.67	1.20±0.14	74.18±6.22	>400	110.20±6.64	5.45±0.12
OVCAR3	11.10±3.74	7.32±4.36	16.60±6.42	>400	38.90±3.11	33.4±0.61
SKOV3	1.59±0.04	1.50±0.02	2.33±0.35	>400	3.92±0.59	8.15±0.12
Hep-G2	4.98±0.66	2.05±0.16	10.05±0.15	>400	12.84±2.97	6.12±0.32
CACO-II	>400	36.41±1.72	316.79±13.01	>400	>400	18.98±0.50
SW620	1.40±0.155	5.51±0.31	44.05±0.84	>400	14.65±2.27	8.63±0.16

Table 7 Cell cycle analysis in SKOV3 cells after exposure to α-mangostin

Time (h)	G0/G1	S	G2/M
0	57.11±3.36	14.08±2.95	27.68±4.16
1	64.65±2.74	9.46±1.03	24.26±2.73
3	75.00±5.21	8.54±3.58	14.90±1.55
6	78.60±3.59	7.79±2.96	12.44±2.81

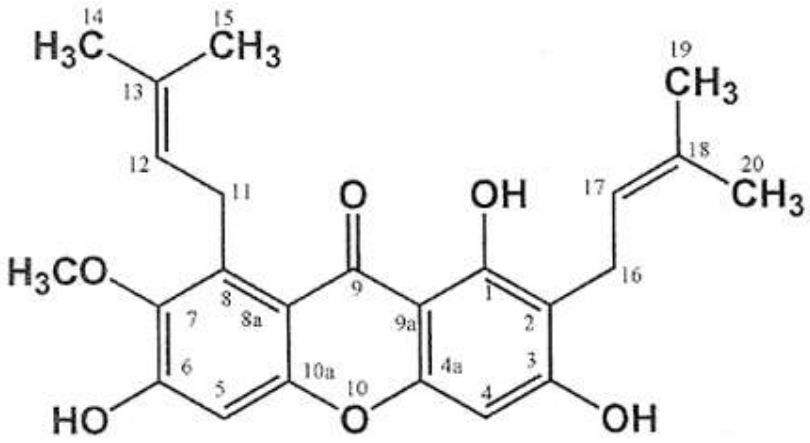

Figure 1 The chemical structure of α-mangostin

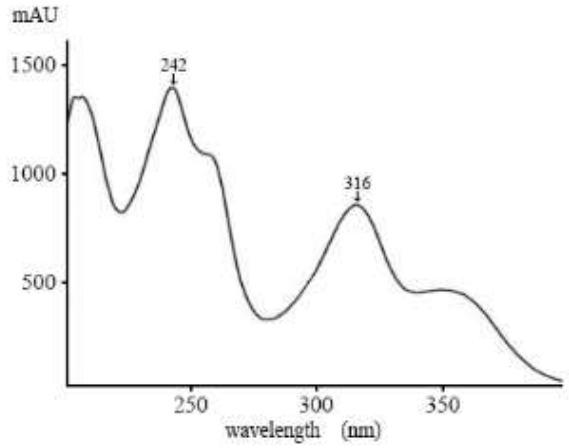

Figure 2 UV spectrum of α-mangostin conducted by UV radiation from 210-370 nm

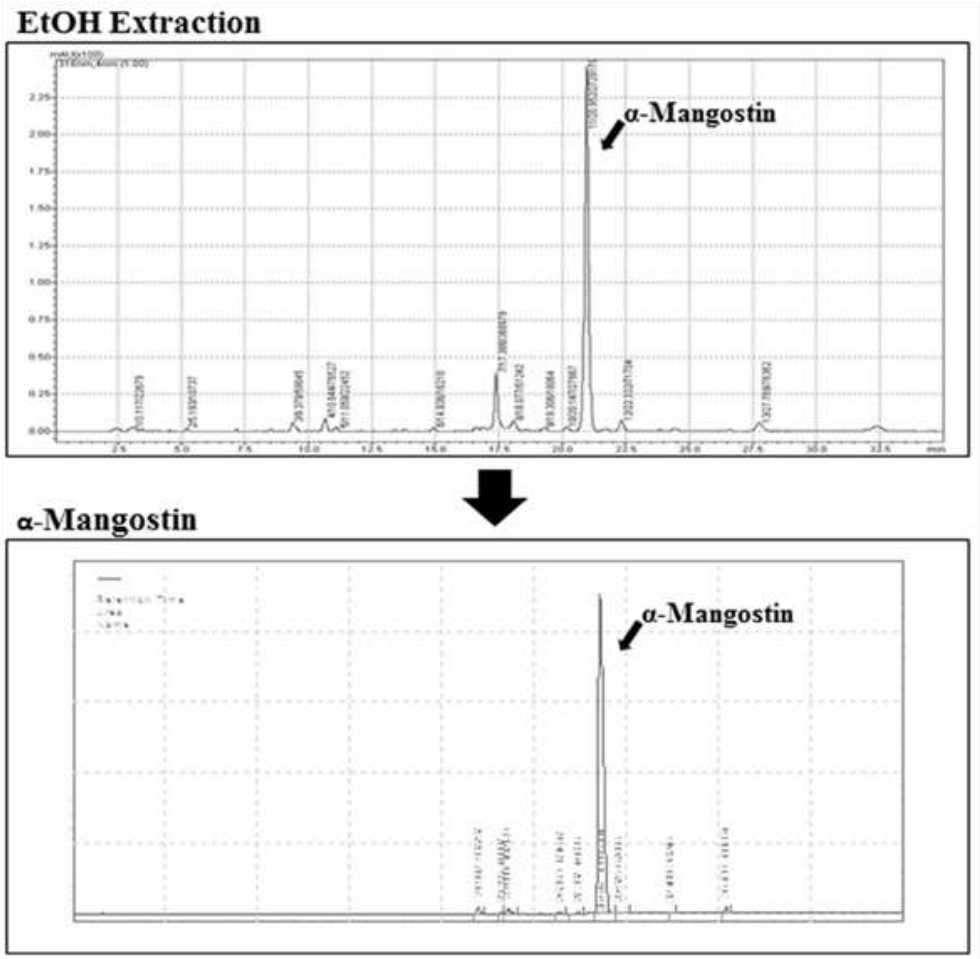

Figure 3 HPLC chromatogram at 316 nm of standard α-mangostin (A), ethanolic crude extract (B) and purified α-mangostin (C)

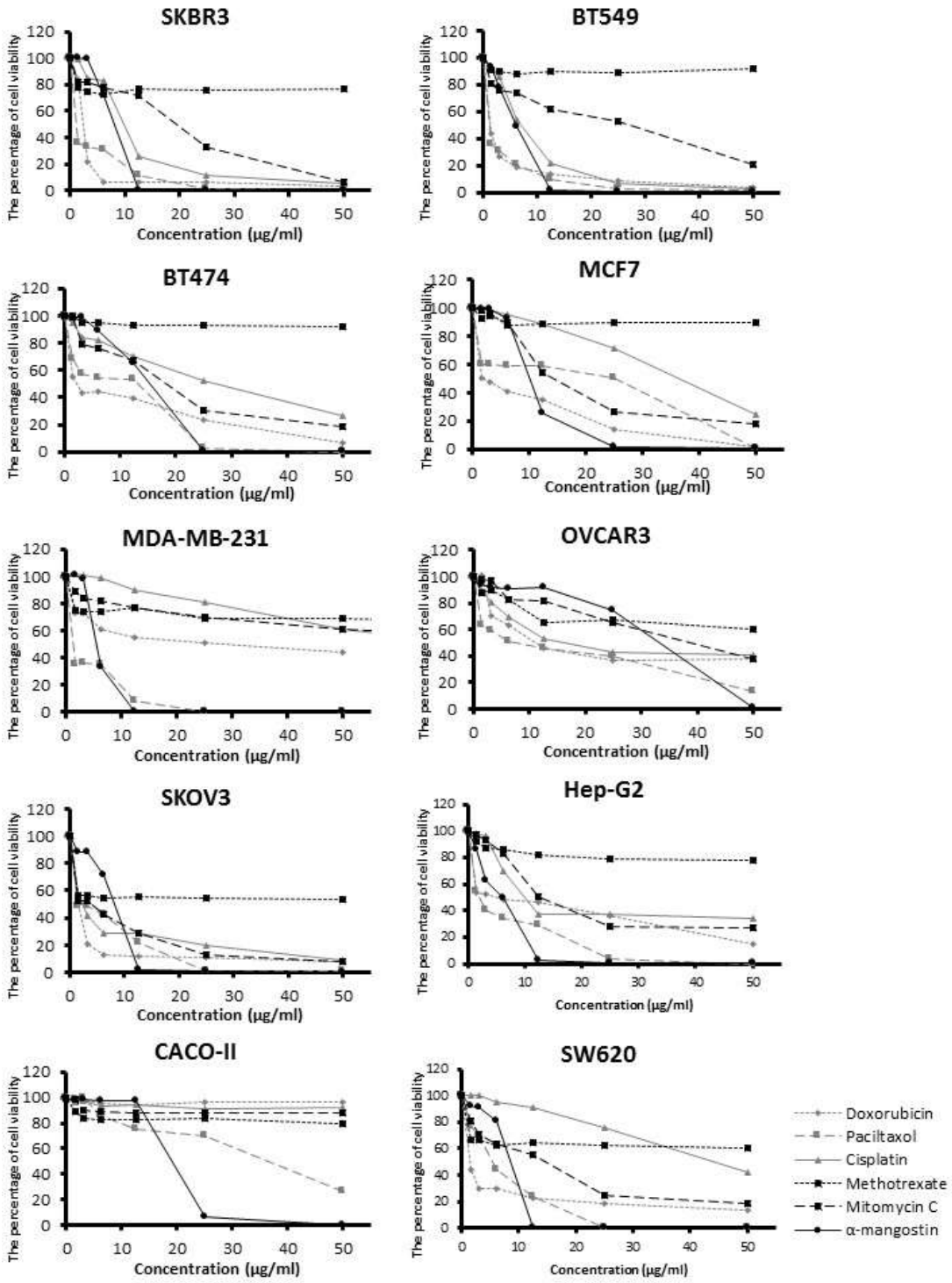

Figure 4 Viability of all cancer cell lines after treated with cytotoxic agents and α-mangostin

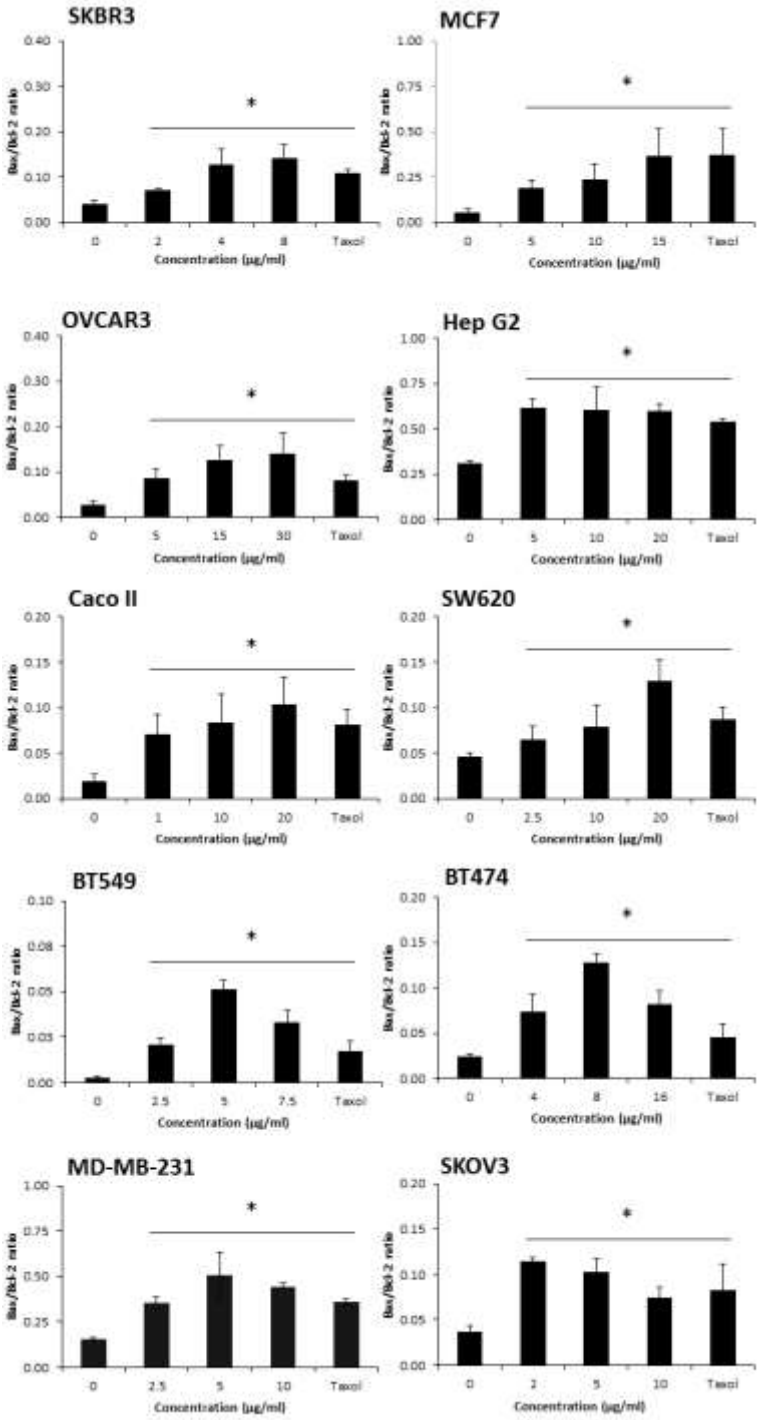

Figure 5 The expression ratio of Bax/Bcl-2 from 10 cancer cell lines treated with various concentrations of α-mangostin, Taxol: a standard anticancer drug as control. The results are mean ± S.E.M. from three independent experiments. *, $p < 0.05$, compared to un-treated α-mangostin.

REFERENCES

1. Ji X et al. Quantitative and qualitative determination of six xanthones in Garcinia mangstana L. by LC-PDA and LC-ESI-MS. J Pharm Biomed Anal 2007; 43: 1270-6.
2. Chairungsrilerd N et al. Mangostanol, a prenyl xanthone from Garcinia mangostana. Phytochemistry 1996; 43: 1099-102.
3. Sakagami Y et al. Antibacterial activity of alpha-mangostin against vancomycin resistant Enterococci (VRE) and synergism with antibiotics. Phytomedicine 2005; 12: 203-8.
4. Matsumoto K et al. Preferential target is mitochondria in alpha-mangostin-induced apoptosis in human leukemia HL60 cells. Bioorganic & Medicinal Chemistry 2004; 12: 5799-806.
5. Williams P et al. Mangostin inhibits the oxidative modification of human low density lipoprotein. Free Radic Res 1995; 23: 175-84.
6. Chairungsrilerd N et al. Pharmacological properties of alpha-mangostin, a novel histamine H1 receptor antagonist. Eur J pharmacol 1996; 314: 351-6.
7. Iinuma M et al. Antibacterial activity of xanthones from guttiferaeous plants against methicillin-resistant Staphylococcus aureus. J Pharm Pharmacol 1996; 48: 861-5.
8. Furukawa K et al. The mode of inhibitory action of α-mangostin, a novel inhibitor, on the sarcoplasmic reticulum Ca2+-pumping ATPase from rabbit skeletal muscle. Jpn J Pharmacol 1996; 71: 337-40.
9. Sato A et al. Alpha-mangostin induces Ca2+-ATPase-dependent apoptosis via mitochondrial pathway in PC12 cells. J Pharmacol Sci 2004; 95: 33-40.
10. Gutierrez-Orozco F, Failla ML. Biological activities and bioavailability of mangosteen xanthones: a critical review of the current evidence. Nutrients 2013; 5:3163-3183.
11. Budavari S et al. Mangostin. In: Budavari S (ed) The Merck index: an encyclopedia of chemicals, drugs and biologicals, 12 edn. Merck Research Laboratories division of Merck and Co., Inc, Whitehouse Satation, NJ, 1996; pp. 978
12. Yoshida A et al. Molecular interactions between phospholipids and mangostin in a lipid bilayer. Colloids Surfaces B: Biointerfaces 1995; 4: 423-32.
13. Chitchumroonchokchai C et al. Anti-tumorigenicity of dietary alpha-mangostin in an HT-29 colon cell xenograft model and the tissue distribution of xanthones and their phase II metabolites. Mol Nutr Food Res 2013; 57: 203-11.
14. Nabandith V et al. Inhibitory effects of crude alpha-mangostin, a xanthone derivative, on two different categories of colon preneoplastic lesions induced by 1, 2-dimethylhydrazine in the rat. Asian Pac J Cancer Prev 2004; 5: 433-8.
15. Shan T et al. alpha-Mangostin suppresses human gastric adenocarcinoma cells in vitro via blockade of Stat3 signaling pathway. Acta Pharmacol Sin 2014; 35: 1065-73.
16. Salomons G et al. The Bax alpha:Bcl-2 ratio modulates the response to dexamethasone in leukaemic cells and is highly variable in childhood acute leukaemia. Int J Cancer 1997; 71: 959-65.
17. Tzifi F et al. The Role of BCL2 Family of Apoptosis Regulator Proteins in Acute and Chronic Leukemias. Adv Hematol 2012; 524308: 1-15
18. Del Poeta G et al. Amount of spontaneous apoptosis detected by Bax/Bcl-2 ratio predicts outcome in acute myeloid leukemia (AML). Blood 2003; 101: 2125-31.
19. Moongkarndi P et al. Comparison of the biological activity of two different isolates from mangosteen. J Pharm Pharmacol 2014; 66: 1171-9.
20. Moongkardi P et al. Antiproliferation, antioxidant and induction of apoptosis by *Garcinia mangostana* (mangosteen) on SKBR3 humanbreast cancer cell line. J Ethnopharmacol 2004; 90: 161-6.
21. Studzinski GP. Cell Growth and Apoptosis: A practical Approach. Oxford University Press, Oxford, UK, 1995; pp.1-19.
22. Suksamrarn S et al. Cytotoxic prenylated xanthones from the young fruit of Garcinia mangostana. Chem Pharm Bull (Tokyo) 2006; 54: 301-5.
23. Nilar, Harrison LJ. Xanthones from the heartwood of Garcinia mangostana. Phytochemistry 2002; 60: 541-8.
24. Mahabusarakam W et al. Chemical constituents of Garcinia mangostana. J Nat Prod 1987; 50: 474-8.
25. Akao Y et al. Anti-cancer effects of xanthones from pericarps of mangosteen. Int J Mol Sci 2008; 9:355-70.
26. Aisha AF et al. α-Mangostin enhances betulinic acid cytotoxicity and inhibits cisplatin cytotoxicity on HCT 116 colorectal carcinoma cells. Molecules 2012; 17:2939-54.
27. Xu Q et al. alpha-Mangostin suppresses the viability and epithelial-mesenchymal transition of pancreatic cancer cells by downregulating the PI3K/Akt pathway. Biomed Res Int 2014; 546353: 1-12.
28. Kurose H et al. Alterations in Cell Cycle and Induction of Apoptotic Cell Death in Breast Cancer Cells Treated with alpha-Mangostin Extracted from Mangosteen Pericarp. Journal of Biomedicine and Biotechnology 2012; 672428: 1-9.
29. Watanapokasin R et al. Effects of α-mangostin on apoptosis induction of human colon cancer. World J Gastroenterol 2011; 17: 2086-95.
30. Shapiro GI, Harper JW. Anticancer drug targets: cell cycle and checkpoint control. The Journal of Clinical Investigation 1999; 104: 1645-53.
31. Lin J. C et al. Induction of apoptosis and cell-cycle arrest in human colon cancer cells by meclizine. Food Chem Toxicol 2007; 45: 935-44.
32. Moongkarndi P et al. Antiproliferation, antioxidation and induction of apoptosis by Garcinia mangostana (mangosteen) on SKBR3 human breast cancer cell line. J Ethnopharmacol 2004; 90: 161-6.
33. Kosem N et al. In vivo toxicity and antitumor activity of mangosteen extract. J Nat Med 2013; 67: 255-63.
34. Burlacu A. Regulation of apoptosis by Bcl-2 family proteins. J Cell Mol Med 2003; 7: 249-57.
35. Czabotar PE et al. Control of apoptosis by the BCL-2 protein family: implications for physiology and therapy. Nat Rev Mol Cell Biol 2014; 15: 49-63.
36. Yang D et al. Apoptosis induced by chamaejasmine in human osteosarcoma cells through p53 pathway. Tumour Biol 2015; 1-7.
37. Ahamed M et al. Comparative cytotoxicity of dolomite nanoparticles in human larynx HEp2 and liver HepG2 cells. J Appl Toxicol 2015; 35: 640-50.
38. Orozco FG et al. Uptake and metabolism of alpha-mangostin by human cell lines: HepG2 liver cells, HT-29 colon cells, and THP-1 macrophage-like cells. The FASEB Journal 2012; 26: 646.17.
39. Bumrungpert A et al. Bioaccessibility, biotransformation, and transport of alpha-mangostin from Garcinia mangostana (Mangosteen) using simulated digestion and Caco-2 human intestinal cells. Mol Nutr Food Res 2009; 53 Suppl 1: S54-61.
40. Liu HF et al. Expression and significance of proapoptotic gene Bax in gastric carcinoma. World J Gastroenterol 1999; 5: 15-7.